

# Enhancement-mode AlGaIn/GaN HEMTs fabricated by fluorine plasma treatment\*

Quan Si(全思)<sup>†</sup>, Hao Yue(郝跃), Ma Xiaohua(马晓华), Xie Yuanbin(谢元斌), and Ma Jigang(马骥刚)

(Key Laboratory of Wide Band Gap Semiconductor Materials and Devices, Institute of Microelectronics, Xidian University, Xi'an 710071, China)

**Abstract:** The fabrication of enhancement-mode AlGaIn/GaN HEMTs by fluorine plasma treatment on sapphire substrates is reported. A new method is used to fabricate devices with different fluorine plasma RF power treatments on one wafer to avoid differences between different wafers. The plasma-treated gate regions of devices treated with different fluorine plasma RF powers were separately opened by a step-and-repeat system. The properties of these devices are compared and analyzed. The devices with 150 W fluorine plasma treatment power and with 0.6  $\mu\text{m}$  gate-length exhibited a threshold voltage of 0.57 V, a maximum drain current of 501 mA/mm, a maximum transconductance of 210 mS/mm, a current gain cutoff frequency of 19.4 GHz and a maximum oscillation frequency of 26 GHz. An excessive fluorine plasma treatment power of 250 W results in a small maximum drain current, which can be attributed to the implantation of fluorine plasma in the channel.

**Key words:** high electron mobility transistors; AlGaIn/GaN; fluorine plasma treatment; threshold voltage

**DOI:** 10.1088/1674-4926/30/12/124002

**PACC:** 7340N; 7360L; 7320

**EEACC:** 2520D; 2530C

## 1. Introduction

AlGaIn/GaN high electron mobility transistors (HEMTs) are excellent candidates for high power and high frequency applications at elevated temperatures owing to their superior material properties<sup>[1-4]</sup>. A high-density two-dimensional electron gas (2DEG) induced by spontaneous and piezoelectric polarization effects<sup>[5]</sup> presents conventional AlGaIn/GaN HEMTs as depletion-mode (D-mode) transistors with a threshold voltage ( $V_{\text{th}}$ ) typically around  $-4$  V. However, the development of AlGaIn/GaN enhancement-mode HEMTs (E-HEMTs) will greatly enhance the versatility of this device technology and extend its applications to the domain of digital circuits. Therefore, there is great interest in the realization of E-mode AlGaIn/GaN HEMTs.

E-HEMTs have been fabricated by a variety of techniques including the growth of a thin barrier layer<sup>[6]</sup>, growth of a pn junction barrier under the gate<sup>[7]</sup>, a recessed-gate structure by etching part of the AlGaIn layer<sup>[8-10]</sup> and fluorine plasma treatment<sup>[11-13]</sup>. The fluorine plasma treatment approach shows facile technology and good control of the threshold voltage<sup>[13]</sup>. In this paper, we report the fabrication of 0.6  $\mu\text{m}$  gate-length E-mode AlGaIn/GaN HEMTs grown by metal organic chemical vapour deposition (MOCVD) on sapphire substrates, and compare and analyze the devices under different fluorine plasma treatment conditions.

## 2. Device structure and fabrication

The AlGaIn/GaN HEMT layer was grown by metal organic chemical vapour deposition on a sapphire substrate. The

heterostructure consists of a nucleation layer, a 1  $\mu\text{m}$ -thick GaN buffer layer and an un-doped 20 nm-thick AlGaIn barrier layer. The AlN mole fraction of the AlGaIn was 30%. From Hall measurements we know that the 2DEG electron mobility and concentration are 1267  $\text{cm}^2/(\text{V}\cdot\text{s})$  and  $1.12 \times 10^{13} \text{ cm}^{-2}$  at room temperature, respectively. Figure 1 shows the structure of our E-mode HEMT.

The wafer was divided into four parts as shown in Fig. 2. One part corresponds to one fluorine plasma treatment condition as shown in Table 1. The implanted region of each part was opened by a step-and-repeat system separately and etched by RIE separately. The device fabrication started with mesa isolation which was formed by ICP with an etch-depth of 200 nm. Ohmic contacts consisting of Ti/Al/Ni/Au (22 nm/140 nm/55 nm/45 nm) were annealed in a nitrogen ambient at 850  $^{\circ}\text{C}$ , yielding a contact resistance typically around 1.0  $\Omega\cdot\text{mm}$ . First, 60 nm-thick  $\text{Si}_3\text{N}_4$  passivation film was deposited on the sample by PECVD. The implanted region of part 1 was opened

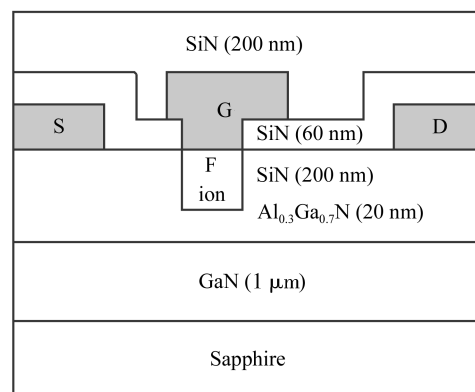


Fig. 1. Cross section of enhancement-mode AlGaIn/GaN HEMT.

\* Project supported by the National Natural Science Foundation of China (No. 60736033).

<sup>†</sup> Corresponding author. Email: siquan@163.com

Received 1 June 2009, revised manuscript received 12 July 2009

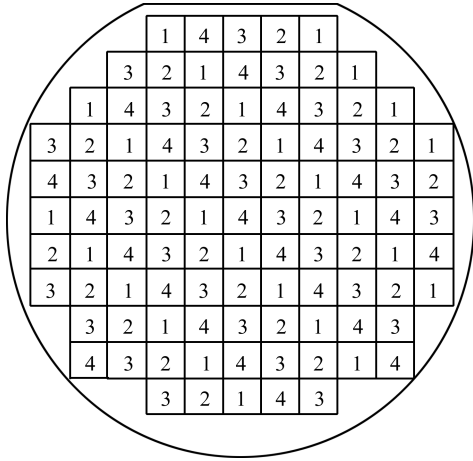


Fig. 2. Four parts divided on the wafer. Each part corresponds to one fluorine plasma treatment condition.

Table 1. Corresponding relation between fluorine plasma treatment condition and wafer part.

Part	Fluorine plasma treatment condition
1	Without fluorine plasma treatment
2	55 W, 150 s
3	150 W, 150 s
4	250 W, 150 s

by the step-and-repeat system and the Si<sub>3</sub>N<sub>4</sub> in the region was etched by reactive ion etching (RIE). Then, the implanted region of part 2 was opened by the step-and-repeat system. Following etching of the Si<sub>3</sub>N<sub>4</sub> under the gate, the wafer was treated by CF<sub>4</sub> plasma (55 W, 150 s) in a reactive ion etching system, and then parts 3 and 4 were opened separately by the step-and-repeat system and etched separately by RIE as for part 2, but with different fluorine plasma RF powers. Gate windows with 0.9 μm gate length were opened by photolithography. Finally, a Ni/Au Schottky gate was deposited by electron-beam evaporation, and a second Si<sub>3</sub>N<sub>4</sub> passivation film with 200 nm-thick was deposited. The direct current characteristics and high frequency characteristics were measured by an Agilent 1500B semiconductor parameter analyzer and an Agilent E8363B network analyzer.

### 3. Results and discussion

The DC transfer and transconductance characteristics of devices treated with different fluorine plasma powers are plotted in Figs. 3(a) and 3(b), respectively. Taking conventional HEMTs without fluorine plasma treatment as the baseline devices, the threshold voltages of all the other fluorine plasma-treated HEMTs are shifted to the positive direction. The higher the plasma power is, the larger the shift in V<sub>th</sub> is. When the plasma power increases, on one hand, fluorine ions obtain a higher energy, and on the other hand, fluorine ion density increases due to the enhanced ionization rate of CF<sub>4</sub>. With a higher energy, fluorine ions can reach a deeper depth closer to the channel. According to Eq. (1)<sup>[12]</sup>, the closer the fluorine ions are to the channel and the more fluorine ions there

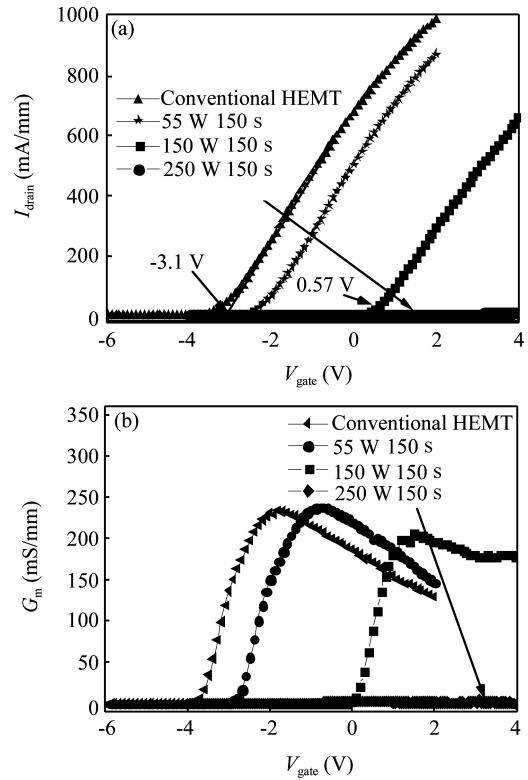


Fig. 3. (a) DC transfer characteristics and (b) transconductance characteristics of devices treated with different fluorine plasma powers.

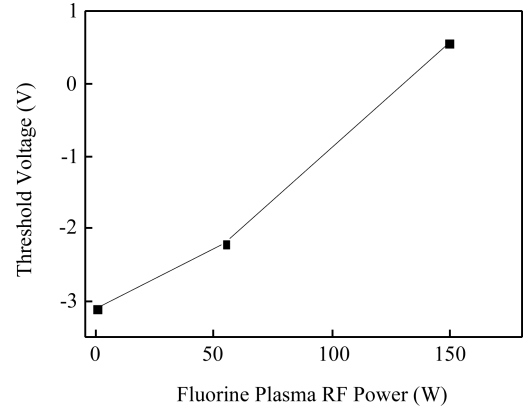


Fig. 4. Dependence of V<sub>th</sub> on fluorine plasma treatment power.

are in the AlGaN barrier layer, the larger the threshold voltage is. Figure 4 shows the dependence of V<sub>th</sub> on the fluorine plasma treatment power. The peak transconductance of the device in part 3 is less than that of the device in part 1, while the peak transconductance of the device in part 2 does not decrease compared with the device in part 1. This indicates that the etching damage of 55 W fluorine plasma treatment does not affect the electron mobility in the channel, but the etching damage of 150 W fluorine plasma treatment has an effect on the electron mobility in the channel.

$$V_{th} = \frac{\phi_B}{e} - \frac{d\sigma}{\varepsilon} - \frac{\Delta E_C}{e} + \frac{E_{f0}}{e} - \frac{e}{\varepsilon} \int_0^d dx \int_0^x (N_{Si}(x) - N_F(x)) dx - \frac{edN'_{st}}{\varepsilon} - \frac{eN_b}{C_b} \quad (1)$$

Equation (1) shows the factors that influence the thresh-

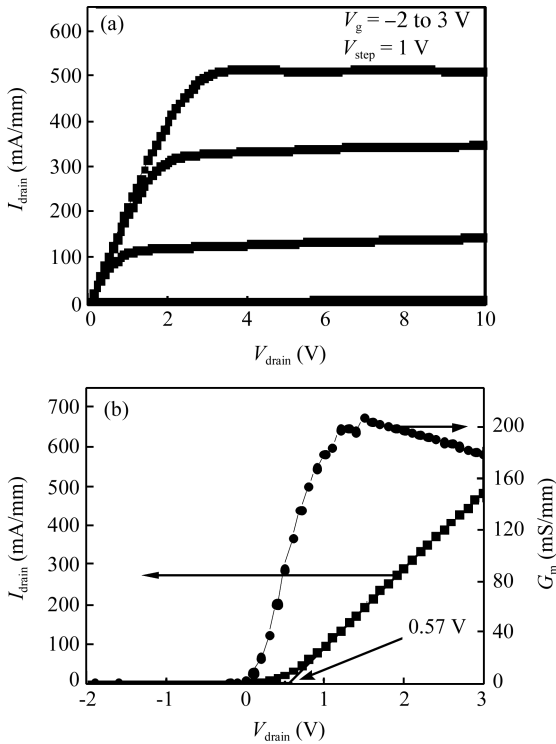


Fig. 5. (a) DC output characteristic and (b) transfer characteristic of the device with a fluorine plasma RF power of 150 W.

old voltage, where  $\Phi_B$  is the metal–semiconductor Schottky barrier height,  $\sigma$  is the overall net (both spontaneous and piezoelectric) polarization charge at the barrier—AlGaIn/GaN interface,  $d$  is the AlGaIn barrier-layer thickness,  $N_{Si}(x)$  is the Si-doping concentration,  $\Delta E_C$  is the conduction-band offset at the AlGaIn/GaN heterojunction,  $E_{f0}$  is the difference between the intrinsic Fermi level and the conduction band edge of the GaN channel,  $\epsilon$  is the dielectric constant of AlGaIn,  $N_{st}$  is the net-charged surface traps per unit area,  $N_b$  is the effective net-charged buffer traps per unit area, and  $C_b$  is the effective buffer-to-channel capacitance per unit area.

However, as fluorine plasma treatment power increases, as in the devices in part 4, fluorine ions reach the channel and GaN buffer layer, and the electron in the channel is deeply depleted by the  $F^-$  ion. The 2DEG is scatted by the  $F^-$  ion implanted in the channel, which leads to a rapid decrease in electron mobility. Therefore, the output current and transconductance are small when  $V_{GS} = 4$  V. The device in part 3 exhibits enhancement-mode characteristics as shown in Fig. 5, with a peak current density of 501 mA/mm, a peak transconductance of 210 mS/mm and a threshold voltage of 0.57 V. The peak transconductance is smaller than that of conventional HEMTs, which can be attributed to the etching damage.

The gate currents of different fluorine plasma treatment power devices are also compared, as shown in Fig. 6; in the forward bias region, the gate current of fluorine-implanted devices is comparable with that of conventional HEMTs. In the reverse bias region, compared to the conventional HEMT without fluorine plasma treatment, the gate-leakage current of all the fluorine plasma-treated devices decreased. Because tunneling is the dominant source of gate-leakage current, a

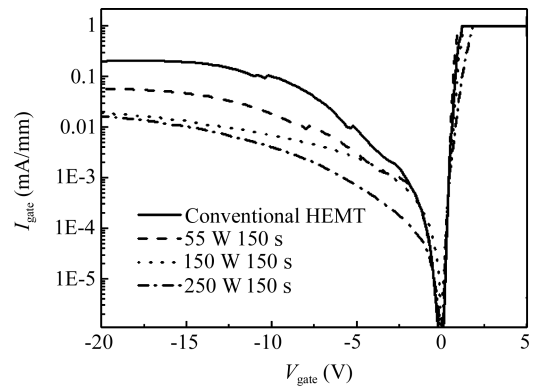


Fig. 6. Gate current of AlGaIn/GaN HEMTs with different fluorine plasma treatment powers.

Table 2.  $f_T$  and  $f_{max}$  of devices treated with different fluorine plasma powers.

Fluorine plasma treatment condition	$f_T$ (GHz)	$f_{max}$ (GHz)
Without fluorine plasma treatment	20.9	31.6
55 W, 150 S	21.3	32.4
150 W, 150 S	19.4	26

decrease in reverse current and no change in forward current indicate that the tunneling width is increased by fluorine plasma treatment, while the barrier height is not changed by fluorine plasma treatment.

RF small-signal characterizations were performed on devices by measuring  $S$ -parameters. Table 2 shows the extrinsic cutoff frequency ( $f_T$ ) and maximum oscillation frequency ( $f_{max}$ ) of devices treated under different conditions. The  $f_T$  and  $f_{max}$  of the device treated by condition 3 are 19.4 GHz and 26 GHz, which is slightly less than that of conventional HEMTs.

### 4. Conclusion

An AlGaIn/GaN enhancement-mode high electron mobility transistor on sapphire substrate has been fabricated by fluorine plasma treatment. Devices treated by different fluorine plasma treatment powers are compared and analyzed. The higher the fluorine plasma RF power is, the larger the threshold voltage is. The devices with 150 W and 150 s fluorine plasma treatment exhibit enhancement-mode characteristics. The devices with 250 W and 150 s fluorine plasma treatment exhibit small output current and small transconductance, which can be attributed to the implantation of a F ion in the channel. Fluorine plasma treatment also results in an increase in the tunneling width, which leads to a decrease in the reverse gate-leakage current.

### References

- [1] Wu Y F, Kapolnek D, Ibbetson J, et al. High Al-content Al-GaN/GaN HEMTs on SiC substrates with very-high performance. IEDM Tech, 1999: 927
- [2] Sheppard S T, Doverspike K, Pribble W L, et al. High power microwave GaN/AlGaIn HEMTs on semi-insulating silicon carbide substrates. IEEE Electron Device Lett, 1999, 20(4): 161

- [3] Kumar V, Lu W, Schwindt R, et al. AlGa<sub>N</sub>/Ga<sub>N</sub> HEMTs on SiC with  $f_T$  of over 120 GHz. *IEEE Electron Device Lett*, 2002, 23(8): 455
- [4] Micovic M, Nguyen N X, Janke P, et al. Ga<sub>N</sub>/AlGa<sub>N</sub> high electron mobility transistors with  $f_T$  of 110 GHz. *Electron Lett*, 2000, 36(4): 358
- [5] Ambacher O, Smart J, Shealy R J, et al. Two-dimensional electron gases induced by Spontaneous and piezoelectric polarization charges in N- and Ga-face AlGa<sub>N</sub>-Ga<sub>N</sub> heterostructures. *J Appl Phys*, 1999, 85(6): 3222
- [6] Akira E, Yoshimi Y, Keiji I, et al. Non-recessed-gate enhancement-mode AlGa<sub>N</sub>/Ga<sub>N</sub> high electron mobility transistors with high RF performance. *Jpn J Appl Phys*, 2004, 43(4B): 2255
- [7] Hu X, Simin G, Yang J, et al. Enhancement-mode AlGa<sub>N</sub>/Ga<sub>N</sub> HFET with selectively grown pn junction gate. *Electron Lett*, 2000, 36(13): 753
- [8] Moon J, Shihchang W, Wong D, et al. Gate-recessed AlGa<sub>N</sub>-Ga<sub>N</sub> HEMTs for high-performance millimeter-wave applications. *IEEE Electron Device Lett*, 2005, 26(6): 348
- [9] Lanford W B, Tanaka T, Otoki Y, et al. Recessed-gate enhancement-mode Ga<sub>N</sub> HEMT with high threshold voltage. *Electron Lett*, 2005, 41(7): 449
- [10] Wang Chong, Zhang Jinfeng, Quan Si, et al. An enhancement-mode AlGa<sub>N</sub>/Ga<sub>N</sub> HEMT with recessed-gate. *Journal of Semiconductors*, 2008, 29(9): 1682
- [11] Cai Y, Zhou Y, Chen K J, et al. High-performance enhancement-mode AlGa<sub>N</sub>/Ga<sub>N</sub> HEMTs using fluoride-based plasma treatment. *IEEE Electron Device Lett*, 2005, 26(7): 435
- [12] Wang R, Wu Y, Chen K J, et al. Gain improvement of enhancement-mode AlGa<sub>N</sub>/Ga<sub>N</sub> high-electron-mobility transistors using dual-gate architecture. *Jpn J Appl Phys*, 2008, 47(4): 2820
- [13] Cai Y, Zhou Y, Lau K M, et al. Control of threshold voltage of AlGa<sub>N</sub>/Ga<sub>N</sub> HEMTs by fluoride-based plasma treatment: from depletion mode to enhancement mode. *IEEE Trans Electron Devices*, 2006, 53(9): 2207